Granular Matter (2010) 12:517–525
DOI 10.1007/s10035-010-0210-y

Discrete element modelling of geomechanical behaviour of methane hydrate soils with pore-filling hydrate distribution

J. Brugada · Y. P. Cheng · K. Soga · J. C. Santamarina

Received: 3 February 2010 / Published online: 25 September 2010
© Springer-Verlag 2010

Abstract Methane hydrate soil is a natural soil deposit that contains methane hydrate in its pores. The micro-scale processes of the geomechanical behaviour of methane hydrate-bearing soils are investigated by the Discrete Element method (DEM). A series of DEM simulations of triaxial compression tests were performed to study the influence of methane hydrate saturation (S_h) on the stress–strain relationship, the volumetric response and on the macroscopic geomechanical properties such as friction and dilation angle. Results of the numerical simulations are compared with laboratory triaxial test data performed on sandy methane hydrate samples. The simulations showed that for the pore-filling case, the hydrate contribution to the strength of the sediment is of a frictional nature, rather than of a cohesive nature.

Keywords Discrete element · Methane hydrates · Pore-filling · Triaxial drained tests

1 Introduction

Methane hydrate soil is a natural soil deposit that contains methane hydrate in its pores. Methane hydrate, which is one form of gas hydrate, is a metastable solid material that consists of methane (CH_4) and water molecules. The water molecules form a structure, in which a floating molecule of methane gas is caged. Typically, 1 m^3 of methane hydrate can release 164 m^3 of methane gas and 0.87 m^3 of water when the hydrate dissociates (i.e. becomes unstable) under standard condition.

Methane hydrate soil can only develop and exist under conditions of high pressure and low temperature (for example, 100 kPa at −80 °C and 2.5 MPa at 0 °C). Hence, natural methane hydrate soils are usually found under deep seabeds (i.e. 1–2 km deep from the sea level and few hundred metres below deep sea floor) or permafrost regions. In such locations, the existence of high pressure and low temperature conditions allows formation of methane hydrate in soil pores.

Methane hydrate soil is highly compacted (i.e. stable) under deposited conditions and is likely to behave as a bonded sedimentary soil with the hydrate acting as bonding agent. However, once the hydrate dissociates (i.e. becomes unstable) due to decrease in pressure and/or increase in temperature, the bonded structure disappears and the soil may behave as unconsolidated material, which may lead to some geotechnical engineering problems. Particular interests that encourage studies of mechanical behaviour of methane hydrate soils are submarine geohazard, such as initiation of marine landslides due to hydrate dissociation [5,19,12], and wellbore stability during methane gas production from the hydrates [6,13,10].

To date, the precise constitutive behaviour of the soil-hydrate structure is not known due to limited mechanical experimental data of the material. Based on the review of mechanical properties of methane hydrate soils by Soga et al. [15], the following characteristics are apparent. (1) The strength of the soil-hydrate material depends on hydrate saturation (S_h), and the hydrate contribution to the strength is of

J. Brugada (✉) · K. Soga
Department of Engineering, University of Cambridge, Trumpington Street, Cambridge CB2 1PZ, UK
e-mail: jb571@cam.ac.uk

Y. P. Cheng
Department of Civil, Environmental and Geomatic Engineering, University College London, Gower Street, London WC1E 6BT, UK

J. C. Santamarina
School of Civil and Environmental Engineering, Georgia Institute of Technology, 790 Atlantic Drive NW, Atlanta, GA 30332-0355, USA

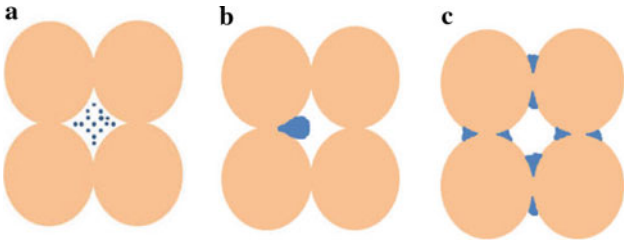

Fig. 1 Pore-scale distribution of methane hydrate:a Pore- lling. b Load-bearingc Cementation

a cohesive nature rather than frictional. (2) The dilation angle is a function of hydrate saturation. (3) The Young's modulus of soil-hydrate formation is higher than that of soil without hydrate, but the Poisson's ratio is found to be independent of hydrate saturation.

Silica sand and sandstone are typical components of sediments, in which natural gas hydrates are observed to form. These minerals (mainly silicate) are not absorbent of large amounts of water and hence gas hydrates would form from water existing originally in the spaces between the particles [16]. Their growth habit can have a profound effect on sediment properties [14]. As shown in Fig. 1, there are three models which describe the microscopic distribution of hydrates in sediments [17]:

(1) pore- lling, Hydrates nucleate on sediment grain boundaries and grow freely into pore spaces without bridging two or more particles together.
(2) load-bearing. Hydrate bridges neighbouring grains and contributes mechanical stability to the granular skeleton by becoming part of the load-bearing framework. Pore- lling hydrate naturally turns into load bearing hydrate at hydrate saturation S_h = 25–40%.
(3) cementation. Hydrates nucleate at inter-granular contacts and the existing soil skeleton structure is cemented.

Hydrate nucleation and growth processes govern which hydrate distribution pattern occurs. Hence different physical properties are expected for identical sediments with equal hydrate saturations. The effect of hydrate pattern on seismic wave velocity, attenuation and small strain stiffness has been reported extensively [17]. On the other hand, there is limited understanding on how hydrate pattern in uences the intermediate and large strain behaviour and the failure condition [15,17]. In this study, the Discrete Element Method (DEM) is used to investigate this problem. This paper describes the results of DEM simulations of triaxial compression tests on granular specimens that contain different hydrate saturations (S_h) in the pores in the form of pore- lling as shown in Fig. 1a. Two different ways of forming this pore- lling pattern are also compared in this paper to show the possible difference in geomechanical behaviour between the laboratory forming hydrates and the natural occurring hydrates

2 Discrete element simulations of methane hydrate-bearing soils

A discrete element code PFC^{2D} [1] was used for the investigation. A series of drained triaxial compression tests were simulated on samples representing sediments with hydrates growing in the pore space. The samples were cylindrical in shape with a diameter of 1.75 mm and a height of 3.5 mm. The "soil" particles were modelled by spherical particles of diameters ranging from 0.1 to 0.25 mm, whereas the "hydrates" were modelled by spherical particles of 0.04 mm.

A number of different techniques for the preparation of discrete element samples are proposed in the literature. The rst method involves simulating the physical sedimentation process by pluviating particles under gravity [7]. The second technique called the 'multi-layer with undercompaction method' has been proposed by Jiang et al. [2] and consists of placing the particles in different layers, compacting layer by layer, generating a homogenous sample. The third technique is the 'radii expansion method' in which the particle radii are generated with an initial reduced size of their nal radii. This last method is incorporated in PFC^{2D} and was used in this research.

The soil sample preparation consisted of creating a uniformly distributed array of particles inside a container. The particles were created initially at half their nal size. The particles radii were then increased by a multiplier to reach their nal desired porosity n of 0.43 while cycling. This is to ensure that no overlapping of particles was produced during the radii expansion process. This method has the advantage of reduced computation time as the energy to be dissipated to reach equilibrium is small and momentum exchange is local.

In order to simulate the formation of hydrates under deep seabed, the sample was isotropically consolidated to an effective stress of 1 MPa and $n = 0.38$ after the initial "soil" sample preparation. Then, the DEM "hydrate" particles were randomly placed inside the pores. During sample preparation when a new hydrate particle was created, the PFC^{2D} code randomly located it inside the container without overlapping with an existing particle. This process was repeated until the total number of speci ed hydrates was created to reach the desired hydrate saturation. Different "hydrate soil" samples were created with different hydrate saturations, as shown in Fig. 2. For the case with hydrate saturation S_h = 20%, for example, $n = 0.329$ before shearing. The simulations run with this sample preparation method are called the "Soil -> Hydrates" cases.

However, methane hydrate soil samples are sometimes created in the laboratory by mixing soil particles with

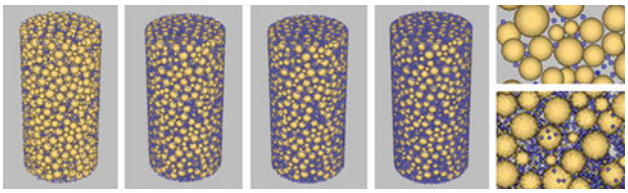

Fig. 2 DEM triaxial samples at different hydrate saturation (S_h = 10, 20, 30, 35%) and detail at the pore scale (S_h = 10, 35%)

Table 1 Material properties used in DEM simulations

Property	Soil	Methane hydrate
Density (kg/m^3)	2,300	900
Particle sizes D (mm)	0.1–0.25	0.04
Contact stiffness E_c (MPa)	286	0.286–28.6
Normal stiffness k_n (N/m)	2DE$_c$	2DE$_c$
Shear stiffness k_s (N/m)	0.7 k_n	0.7 k_n
Inter-particle friction μ	0.75	0.75

synthetic hydrate. To simulate such condition, "hydrate" particles were randomly placed in the pore space immediately after the "soil" sample reached a state of equilibrium under zero con nement. The mixture of "soil" and "hydrate" particles was then isotropically consolidated to an effective stress of 1 MPa. For the case with hydrate saturation S_h = 20%, $n = 0.36$ before consolidation and $n = 0.323$ before shearing. The simulations run with this sample preparation method are called the "Soil + Hydrate" cases.

The two cases of "hydrate-soil" samples were then sheared by applying a constant velocity to the top platen of 1×10^{-10} m/s. In order to ensure that a steady-state solution was reached, the differential density scaling scheme of PFC[35] was used in the simulations. The con ning pressure of 1 MPa was kept constant throughout the shearing process by adjusting a numerical servo-mechanism.

The material densities used in the DEM simulations correspond to those characterized from Nankai Trough[9,15]. The particle size distribution for the soil corresponds to the one described by Masui et al.[8]. The normal stiffness of the soil particles (k_n) was varied according to its particle diameter to keep the elastic contact stiffness of the soil grain to be constant (E_c = 286 MPa, where $E_c = k_n/2D$, [1]). The elastic contact stiffness of the hydrate particles (E_{chyd}) was varied between 0.286 and 28.6 MPa in order to examine the effect of hydrate stiffness on the mechanical behaviour. A summary is shown in Table 1. The smooth lateral cylindrical wall was given a normal stiffness of one tenth of the mean particle stiffness (K_{nw} =1e4 N/m, $K_{sw} = 0$ N/m, μ_w =0) in order to simulate a soft con nement. Gravity was not specified.

3 Simulated stress–strain behaviour

The simulated deviator stress-axial strain curves from some simulations are shown in Fig. 3. The "Soil + Hydrate" cases are shown in Fig. 3a, whereas the "Soil->Hydrate" cases are shown in Fig. 3b. For each case, simulation results with five different hydrate saturations (S_h = 0, 10, 20, 30 and 35%) are shown. The simulations correspond to the case when the ratio of the contact stiffness of the hydrate particles to that of the soil particles (E_{chyd}/E_{csoil}) is fixed to be 0.1 (the effect of (E_{chyd}/E_{csoil}) on the mechanical behaviour is discussed in Sect. 6).

In "Soil + Hydrate" samples, the shear strength (the maximum deviator stress) increased with hydrate saturation from 1.35 MPa (S_h = 0%) to 1.76 MPa (S_h =35%). In

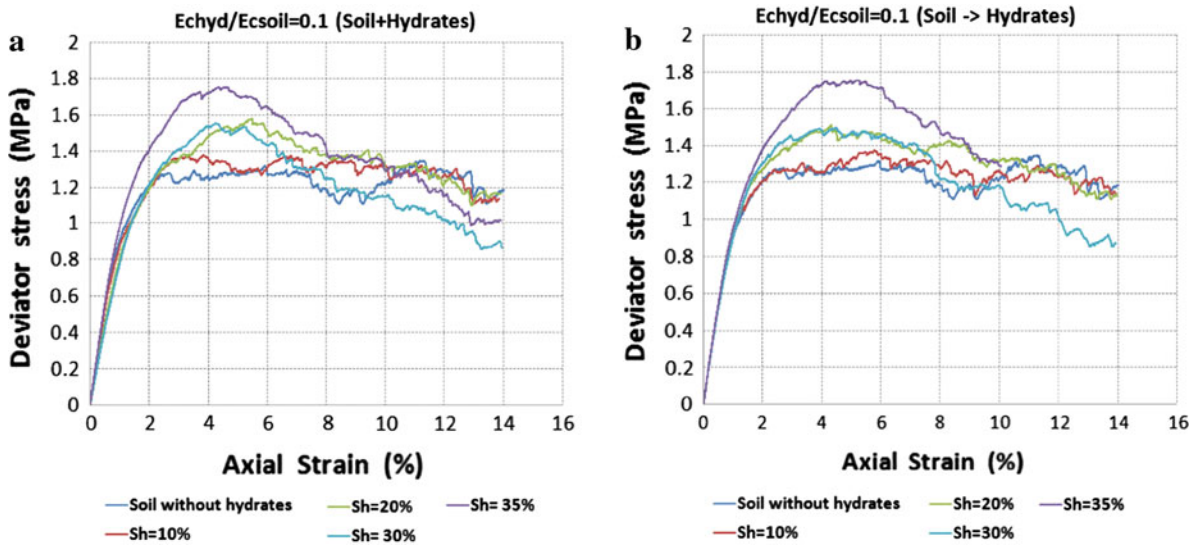

Fig. 3 Effect of hydrate saturation (S_h) on shear strength: a "Soil + Hydrate" cases; b "Soil->Hydrate" cases

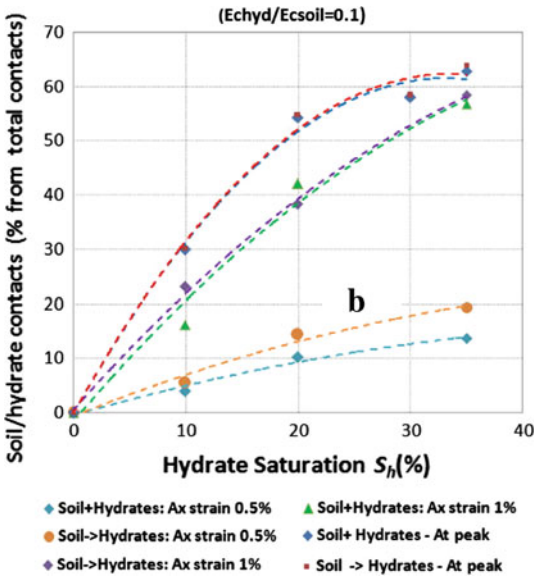

Fig. 4 Percentage of soil/hydrate contacts

"Soil->Hydrate" samples, the shear strength increased from 1.35 MPa ($S_h = 0\%$) to 1.78 MPa ($S_h = 35\%$). The deviator stress tends to converge to a value of 1.2 MPa, at an axial strain of about 14% for hydrate saturations below 20%. Figure 3 shows the stress–strain relationship with different hydrate saturations for the two samples, indicating that the effect of sample preparation on shear resistance is negligible. The shear resistance is primarily due to grain–grain interactions. An analysis of the number of hydrates in contact with soil particles at peak shear strength, showed that as the hydrate saturation increased from $S_h = 10$ to 35%, the percentage of hydrate particles in contact with soil particles (relative to the total number of contacts) increased from 30 to 63% respectively, as shown in Fig. 4. This result is the same for the two cases ("Soil + Hydrate", "Soil->Hydrate") reinforcing the observation that the effect of sample preparation on shear resistance is negligible, probably because the stiffness of the hydrate particles is much smaller than that of the soil particles.

The secant Young's modulus (E_{sec}) generally increased with hydrate saturation. The rate of increase of E_{sec} was higher at larger values of axial strain, as shown in Fig. 5. It can be observed in Fig. 3 that the effect of hydrate saturation (S_h) on initial stiffness is greater in the "Soil + Hydrate" case than in the "Soil->Hydrate" case. The effect of the hydrates is shown at an early stage for the "Soil + Hydrate" case. As shown in Fig. 4, for hydrate saturation of $S_h = 35\%$, and axial strain of 0.5%, the percentage of soil/hydrate contacts is 13% for the "Soil + Hydrate" case and 20% for the "Soil->Hydrate" case, resulting in slightly lower secant Young's modulus for the "Soil + Hydrate" case at low values of axial strain.

The DEM results presented here are qualitatively similar to the results of drained triaxial compression tests carried out by Masui et al. [8] on samples of Toyoura sand with different hydrate saturations. They created pore- lling gas hydrates synthetically by growing methane hydrate in a mixture of sand and ne ice particles below ice melting point. The percolation of hydrate occurred at an initial con ning pressure of 1 MPa. The pore pressure was increased at the increment rate of 0.5–1 MPa per minute until it reached the induction pressure of 8 MPa with a con ning pressure of 9 MPa. This process forms hydrate mainly inside the soil pores. Soil samples with different methane hydrate saturations can be created by changing the induction period. Masui et al. [8] found that the strength of the sample increased significantly only after hydrate saturation was above $S_h = 26\%$ as shown in Fig. 6. The results of the DEM simulations showed that the shear strength increased only after the hydrate saturation reached $S_h = 20\%$. Masui et al. [8] also observed strain softening behaviour for samples with hydrate saturation in excess of $S_h = 37\%$. In our

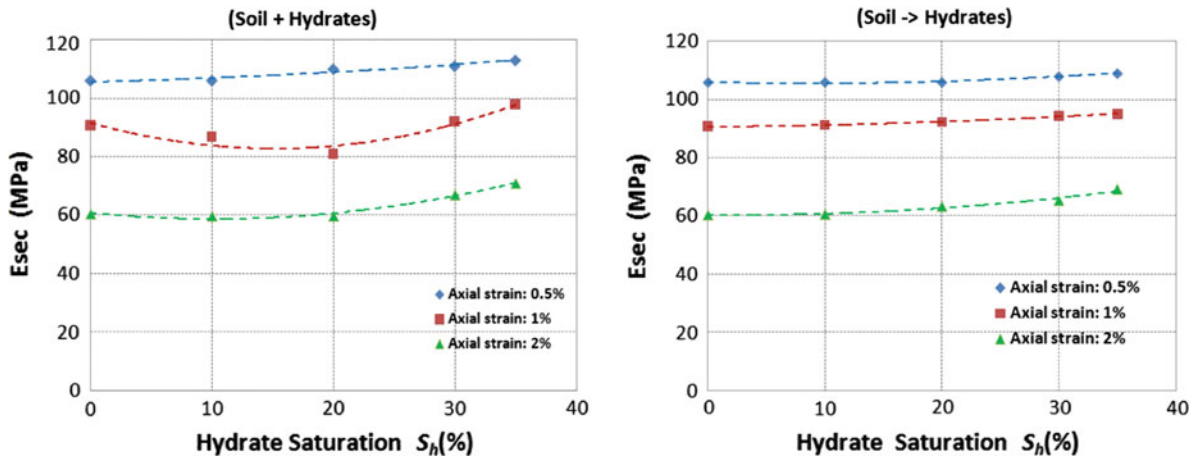

Fig. 5 Secant Young's modulus (E_{sec}) vs Hydrate saturation (S_h)

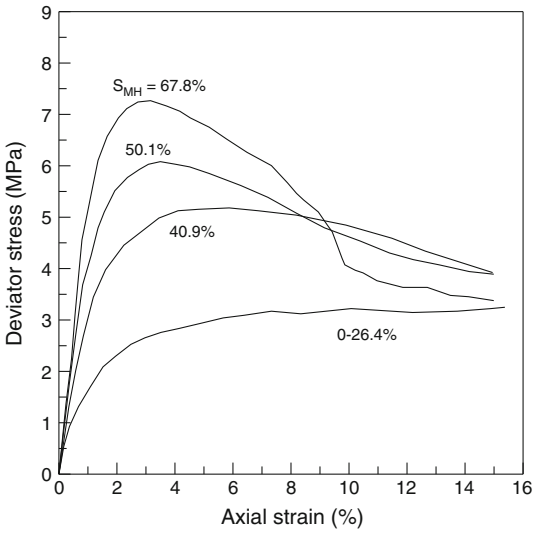

Fig. 6 Stress–strain results from drained triaxial tests on Toyoura sand [15]

study, strain-softening behaviour was observed when hydrate saturation was above $S_h = 30\%$

Hydrates in the pore- lling case are formed inside the soil pores rather than at the particle contacts. They occlude the pores but do not contribute to the strength of the soil when the hydrate saturation is small. This was con rmed by an analysis of the percentage of hydrate particles involved in the strong force network of the sediment (particles with normal contact force equal or larger than the mean normal contact force). The percentage of hydrates involved in the strong force network is below 1% for hydrate saturation of $S_h = 10\%$, as shown in Fig. 7. This con rms the observation that hydrates do not contribute to the strength of the sediment for hydrate saturations below $S_h = 20\%$. The analysis also showed that the contribution of hydrates to the strong force network increases at larger values of axial strain.

4 Volumetric response during triaxial compression

A series of simulations were carried out at ve different hydrate saturations (S_h = 0, 10, 20, 30 and 35%) and under con ning pressure of 1 MPa, for the "Soil + Hydrate" and the "Soil->Hydrate" cases. Similarly to the simulated stress–strain behaviour, the sample preparation method was negligible for the volumetric response, as shown in Fig. 8. The results show that the presence of methane hydrate has an effect in the volumetric behaviour of soil: the dilation is enhanced as hydrate saturation increases. All samples exhibit an initial contractive behaviour followed by dilation, as shown in Fig. 8.

The dilation angles at large strain are plotted against hydrate saturation in Fig. 9a. The trend of the DEM simulations is similar to that observed in laboratory tests as shown in Fig. 9b. The dilation angle increases with hydrate saturation, however the increase is more apparent when the hydrate saturation is above S_h = 30%. The simulations also showed that the dilation angle decreases with increasing con ning pressure. Poission's ratio, which is related to the initial slope of the volumetric strain curve remained constant at a value of 0.5.

The maximum compressive volumetric strain at the beginning of shearing increases for higher values of con ning pressure, as shown in Fig. 10. In general, the maximum compressive volumetric strain decreased as hydrate saturation increased.

5 Effect of con ning pressure

Simulations were carried out for samples at con ning pressures of 1, 2 and 3 MPa for the Soil->Hydrate case. Figure 11 shows the stress–strain relationship and the volume change behaviour at three different con ning pressures.

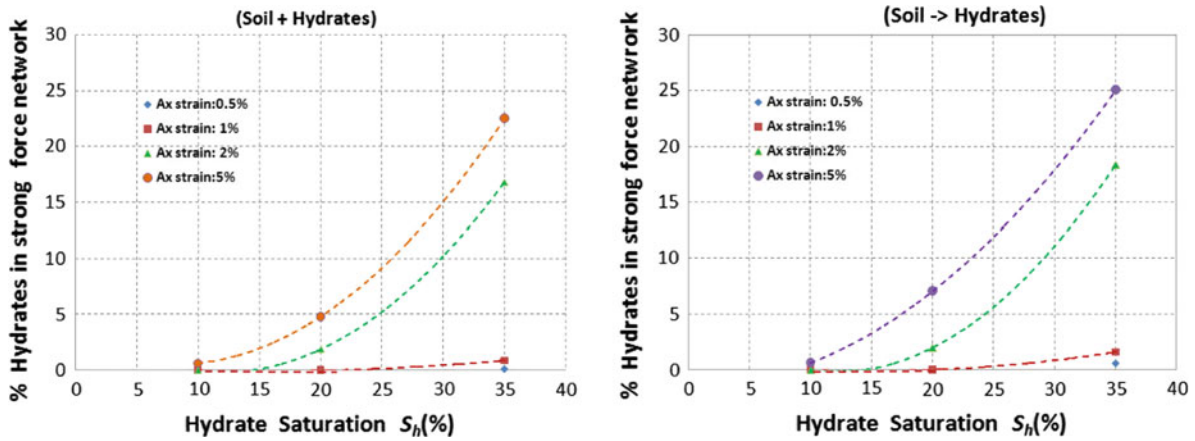

Fig. 7 Percentage of hydrates in strong force network

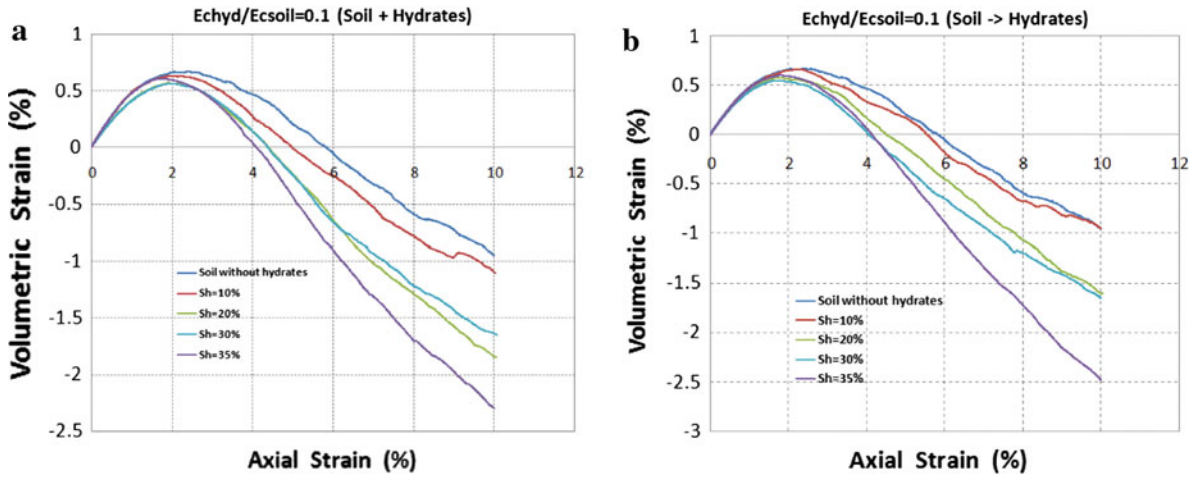

Fig. 8 Effect of hydrate saturation (S_h) on volumetric response: a Soil + Hydrate cases b Soil->Hydrate cases

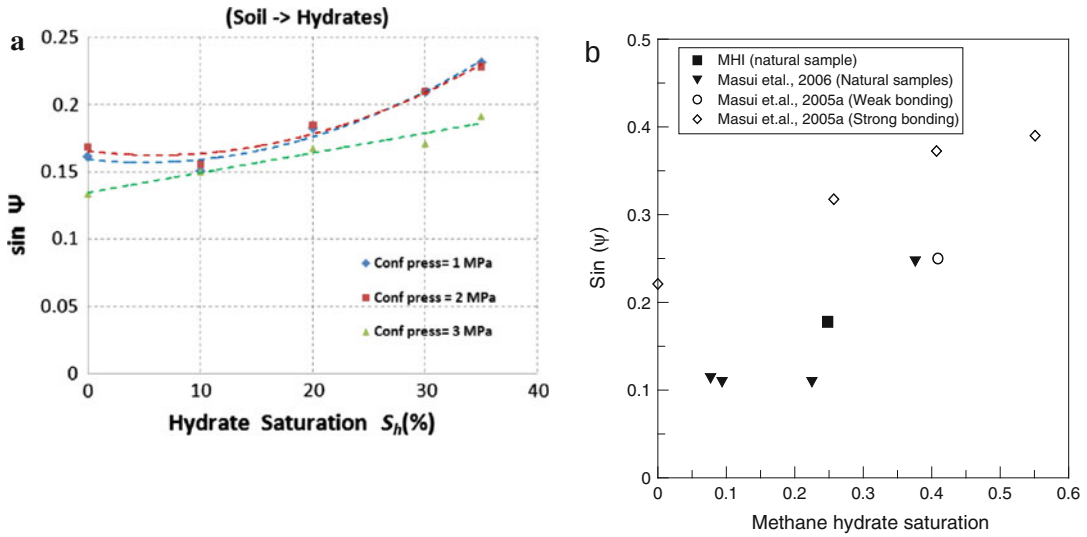

Fig. 9 Relationship between dilation angle and hydrate saturation (S_h): a DEM tests b Data reported by Soga et al. [15]

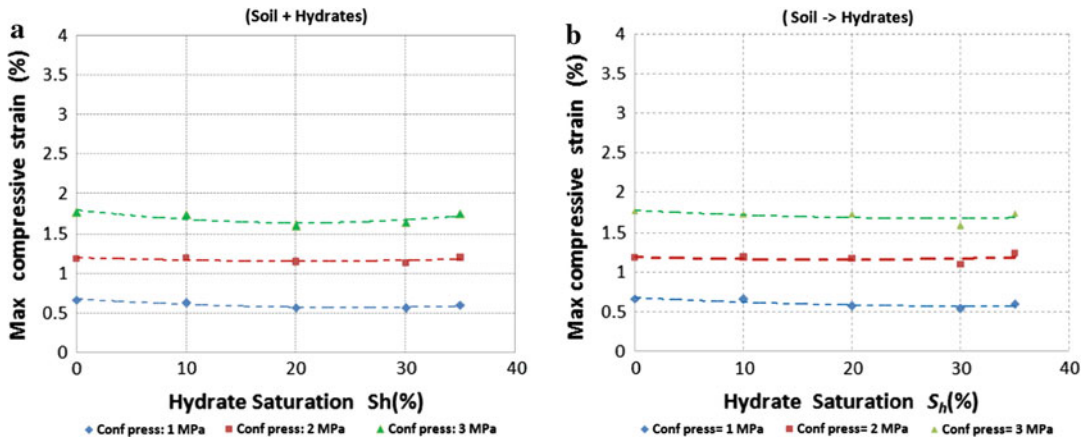

Fig. 10 Maximum compressive volumetric strain vs Hydrate saturation (S_h): a Soil + Hydrate b Soil->Hydrate cases

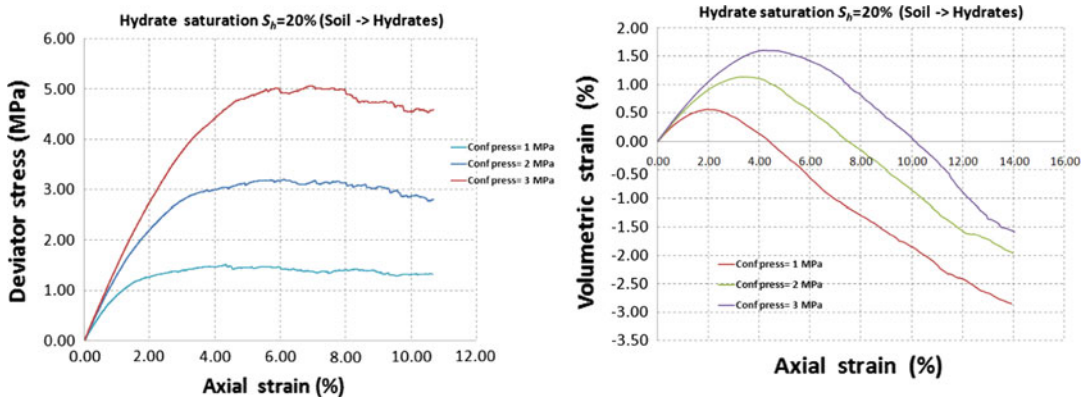

Fig. 11 Effect of con ning pressure on stress–strain and volumetric response

The results show that the con ning pressure has an in uence in the mechanical behaviour of the sample. The shear strength increased approximately 300% from a con ning pressure of 1–3 MPa. The elastic modulus increased from 99 MPa for a con ning pressure of 1–141 MPa for a con ning pressure of 3 MPa. The volumetric response is also in uenced by con ning pressure, with an increase of compressive volumetric strain as the con ning pressure increases. The dilation angle at large strain decreased from 5.1° for a con ning pressure of 1 MPa to 0.9 °C for a con ning pressure of 3 MPa.

Soga et al. [15] reported that the friction angle remained independent of the hydrate saturation on a large number of tests on synthetic soil samples, while cohesion changed as a function of hydrate saturation as shown in Fig. 12c. The range of variation of friction angle for the DEM simulations

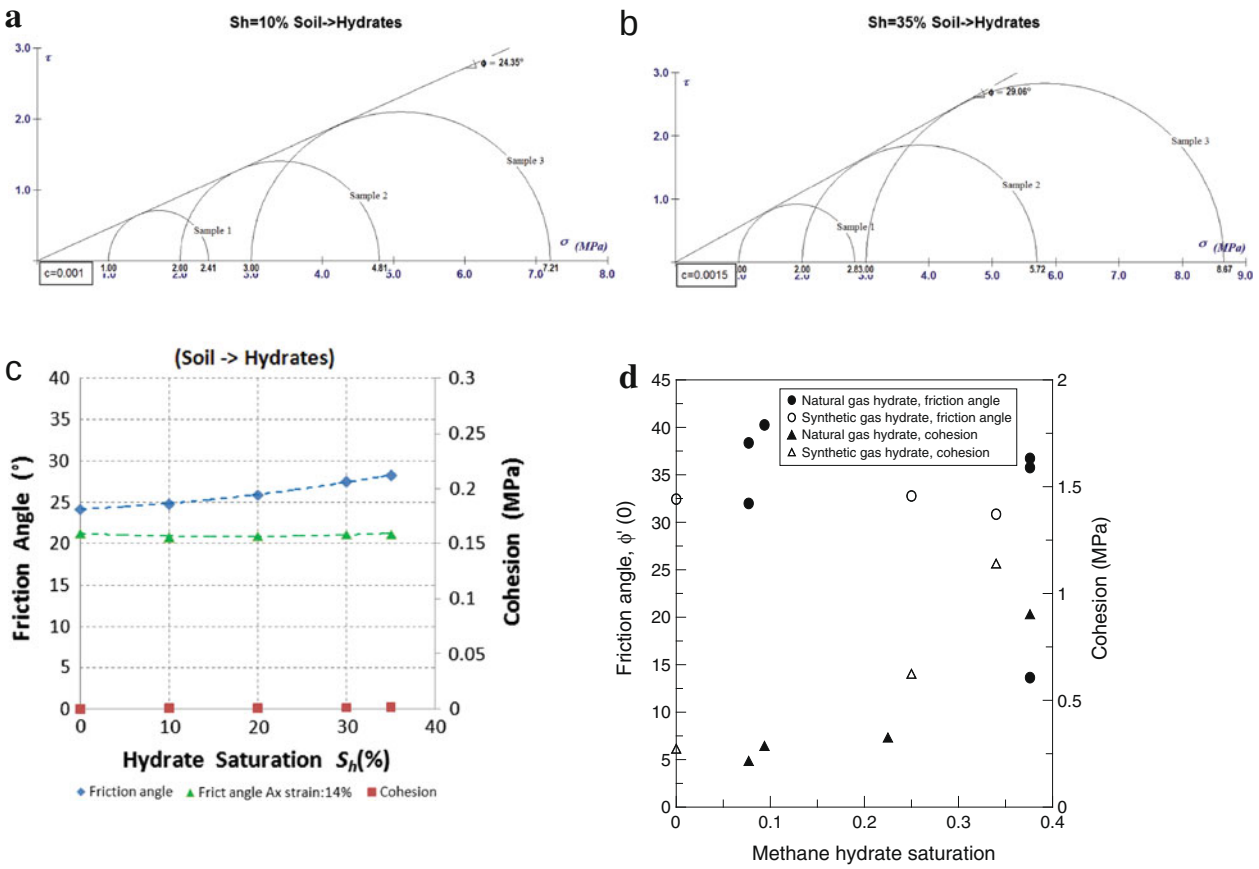

Fig. 12 Variation of friction angle and cohesion vs Hydrate saturation (S_h) for: a–c DEM simulations, d Data reported by Soga et al. [15]

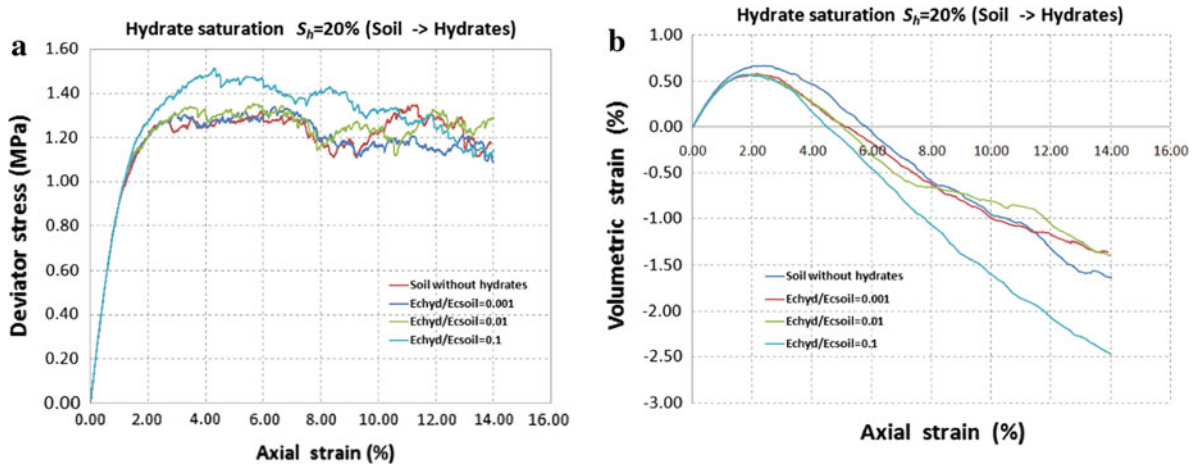

Fig. 13 Stress–strain and volumetric behaviour for $E_{chyd}/E_{csoil} = 0.001$–0.1

with hydrate-soil contact stiffness ratio $E_{chyd}/E_{csoil} = 0.1$ is shown in Fig. 9a, b. The peak friction angle increased from 24° ($S_h = 0\%$) to 28° ($S_h = 35\%$), while the friction angle at axial strain of 14% remained constant at approximately 21°. The value of cohesion remained independent of hydrate saturation. The results suggest that for the pore- lling case, the hydrate contribution to the strength is of a frictional nature, rather than of a cohesive nature.

6 Effect of hydrate-soil contact stiffness ratio

There is a lack of data in the literature regarding the elastic contact stiffness of hydrate particles (E_{chyd}). The value of hydrate contact stiffness is not reported in laboratory experiments performed in natural or synthetic samples of hydrate-bearing soils.

In order to study the effect of hydrate contact stiffness on the behaviour of hydrate-bearing soil, simulations were performed varying the hydrate-soil contact stiffness ratio from 0.001 to 0.1, for samples at different hydrate saturations. As shown in Fig. 13, the contribution of hydrates to the stress–strain appeared only when the hydrate-soil contact stiffness ratio reached a value of 0.1. In terms of the volumetric response, the presence of hydrates produced a reduction in maximum volumetric compressive strain for the whole range of hydrate-soil contact stiffness tested. However the dilation was enhanced only when the hydrate-soil contact stiffness reached 0.1. Further work is needed to evaluate the mechanical properties of hydrates.

7 Conclusions

The results of the DEM simulations show similar trends to the laboratory measured results reported by Soga et al. [15]. The shear strength increases when the hydrate saturation is higher than $S_h = 20\%$. The simulations also showed, that for the pore- lling case, the hydrate contribution to the strength of the sediment is of a frictional nature, rather than of a cohesive nature.

The results showed that the shear strength remained independent of the sample preparation methods examined in this study. However, the "Soil + Hydrate" case tends to show more an effect on the initial stiffness of the sediment compared to the "Soil->Hydrate" case.

The simulations show that the presence of methane hydrate has an effect in the volumetric behaviour of soil, the dilation is enhanced as hydrate saturation increases. The dilation angle decreases with increasing con ning pressure and that the maximum volumetric compressive strain increases for higher values of con ning pressure

The hydrate-soil contact stiffness ratio (E_{chyd}/E_{csoil}) has an important effect on the stress–strain relationship and on the volumetric response of hydrate-bearing soils. The results showed that the contribution of hydrates to the stress–strain relationship appeared only when the hydrate-soil contact stiffness ratio reached a value of 0.1. However further investigation is needed since there is a lack of data in the literature regarding the contact stiffness of hydrate particles (E_{chyd}). Future research will be carried out on the effect of other hydrate growth patterns (cementation, load-bearing) on the

geomechanical behaviour of hydrate-bearing soils. Cementation will be simulated by attaching hydrate particles near soil particle contacts (eg. Wang et al. [18]) and using a simple contact bond model with tensile and shear resistance (eg. Jiang et al. [3,4])

Acknowledgments This work is nancially supported by CONACYT (National Council of Science and Technology, Mexico).

References

1. Itasca: "PFC^{3D}: Particle ow code. User's guide", *version 3.0.*, Minneapolis, USA (2003)
2. Jiang, M., Konrad, J.M., Leroueil, S.: An ef cient technique for generating homogeneous specimens for DEM studies. Comput. Geotech. 30, 579–597 (2003)
3. Jiang, M., Leroueil, S., Konrad, J.M.: Yielding of microstructured geomaterial by Distinct Element Method analysis. J. Eng. Mech. ASCE 131(11), 1209–1213 (2005)
4. Jiang, M., Yu, H.S., Leroueil, S.: A simple and ef cient approach to capturing bonding effect in naturally microstructured sands by discrete element method. Int. J. Numer. Methods Eng. 69, 1158–1193 (2007)
5. Kayen, R.E, Lee, H.J.: Pleistocene slope instability of gas hydrate-laden sediment on the Beaufort Sea Margin. Proceedings 3rd Biot Conference on Poromechanics, vol. 10, pp. 125–141 (1991)
6. Klar, A., Soga, K., Ng, M.Y.A.: Coupled deformation- ow analysis for methane hydrate wells. pp. 652–659. Marine Geotechnology, Oklahoma (2005)
7. Marketos, G.: An investigation of crushing and compaction bands in granular material. PhD Thesis, University of Cambridge (2007)
8. Masui, A., Haneda, H., Ogata, Y., Aoki, K.: The effect of saturation degree of methane hydrate on the shear strength of synthetic methane hydrate sediments. Proceedings of the 5th Int. Conf. on Gas Hydrates. June 13-16, Trondheim, Norway. Paper No. 2037 (2005)
9. Masui, A., Haneda, H., Ogata, Y., Aoki, K.: Triaxial Compression test on submarine sediment containing methane hydrate in deep sea off the coast off Japan. Proceedings of the 41st Annual Conference, Japanese Geotechnical Society (2006)
10. Ng, M.Y.A., Klar, A., Soga, K.: Coupled soil deformation- ow-thermal analysis of methane production in layered methane hydrate soils. OTC 19364, Offshore Technology Conference (2008)
11. Methane Production in Layered Methane Hydrate Soils. OTC 19364, Offshore Technology Conference (2008)
12. Nixon, MF, Grozic, JLH: Submarine slope failure due to hydrate dissociation: A preliminary quanti cation. Can Geotech. J. 44, 314–325 (2007)
13. Rutqvist, J., Moridis, G., Grover, T., Collett, T.: Geomechanical response of known permafrost hydrate deposits to depressurization-induced production. 6th International Conference on Gas Hydrates, Chevron, Vancouver, BC, Canada. Paper No. 5726 (2008)
14. Santamarina, J.C., Yun, T.S.: Hydrate-bearing sediments: Crystal Growth in Granular Materials, Granular matter, In print (2008)
15. Soga, K., Lee, S.L., Ng, M.Y.A., Klar, A.: Characterisation and engineering properties of methane hydrate soils. Characterisation and Engineering Properties of Natural Soils, vol 4, pp 2591– 2642. Taylor and Francis, London (2006)
16. Uchida, T., Takeya, S., Chuvilin, E.M., Ohmura, R.: Decomposition of Methane Hydrates in Sand, Sandstone, Clays and Glass Beads (CH4 Hydrate Decomposition in Sediments). J. Geophys. Res. Solid Earth (Chem. Phys. Miner. Rocks/Volcanology) 109(B5), B05206 (2004)
17. Waite, W.F., Santamarina, J.C., Cortes, D.D., Dugan, B., Espinoza, D.N., Germaine, J., Jang, J., Jung, J.W., Kneafsey, T., Shin, H.S., Soga, K., Winter, W., Yun, T.S.: Physical properties of hydrate-bearing soils. Rev. Geophys. 47, In print (2009)
18. Wang, Y.H., Leung, S.C.: A particulate-scale investigation of cemented sand behavior. Can. Geotech. J. 45, 29–44 (2008)
19. Xu, W., Germanovich, L.N.: Excess pore pressure resulting from methane hydrate dissociation in marine sediments: A theoretical approach. J. Geophys. Res. 111, B01104 (2006)